

## Structural properties of Cd–Co ferrites

S P DALAWAI<sup>a,\*</sup>, T J SHINDE<sup>b</sup>, A B GADKARI<sup>c</sup> and P N VASAMBEKAR<sup>a</sup>

<sup>a</sup>Department of Electronics, Shivaji University, Kolhapur 416 004, India

<sup>b</sup>Department of Physics, KRP Kanya Mahavidyalaya, Islampur 416 409, India

<sup>c</sup>Department of Physics, GKG college, Kolhapur 416 012, India

MS received 6 January 2012; revised 6 June 2012

**Abstract.** Ferrite samples with composition,  $\text{Cd}_x\text{Co}_{1-x}\text{Fe}_2\text{O}_4$  ( $x = 0.80, 0.85, 0.90, 0.95$  and  $1.0$ ), were prepared by standard ceramic method and characterized by XRD, IR and SEM techniques. X-ray analysis confirms the formation of single phase cubic spinel structure. Lattice constant and grain size of the samples increase with increase in cadmium content. Bond length (A–O) and ionic radii ( $r_A$ ) on A-sites increase, whereas bond length (B–O) and ionic radii ( $r_B$ ) on B-site decrease. The crystallite sizes of the samples lie in the range of 29.1–42.8 nm. IR study shows two absorption bands around  $400\text{ cm}^{-1}$  and  $600\text{ cm}^{-1}$  corresponding to tetrahedral and octahedral sites, respectively.

**Keywords.** Cd–Co ferrites; X-ray analysis; infrared spectroscopy; scanning electron microscopy.

### 1. Introduction

The spinel ferrites are extensively used in electromagnetic devices such as memories, sensors and microwaves in modern information technology applications. They possess special magnetic and electrical properties with high chemical stability and mechanical hardness. Cobalt ferrites are in demand, due to these properties, for magnetic recording devices, magneto-optical recording and electronic devices (Gaikwad *et al* 2011). The structural, electrical and magnetic properties of these spinel ferrites are dependent on magnetic interaction and distribution of cations among tetrahedral (A) and octahedral (B) sites (Gabal and Ata-Allah 2004).

The crystallization in ferrites occurs in normal spinel and inverse spinel structures. The cadmium ferrite (with  $\text{Cd}^{2+}$  and  $\text{Fe}^{3+}$  ions on tetrahedral (A) and octahedral (B) sites) and cobalt ferrite (with  $\text{Co}^{2+}$  and  $\text{Fe}^{3+}$  ions on A and B sites) are examples of normal and inverse spinel structures, respectively (Gabal and Ata-Allah 2004). The resistivity of Co ferrites is reported to be higher than that of Cd ferrites. It is found to be dependent on saturation magnetic moments of the samples (Vasambekar *et al* 1999). Abdeen *et al* (2002) studied structural, electrical and transport phenomena of Cd–Co ferrites to report increase in lattice parameter and X-ray density with  $\text{Cd}^{2+}$  contents, while decrease in porosity. Nikumbh *et al* (2001) found change in crystallization phenomenon in  $\text{CdFe}_2\text{O}_4$  ferrite from normal spinel to inverse spinel structure due to addition of Co.

In the present communication, we report structural properties of Cd–Co ferrites.

### 2. Experimental

Polycrystalline spinel ferrites with chemical formula,  $\text{Cd}_x\text{Co}_{1-x}\text{Fe}_2\text{O}_4$  ( $x = 0.80, 0.85, 0.90, 0.95$  and  $1.0$ ) were prepared by the standard ceramic method. The starting materials were of AR grade cadmium oxide (Himedia), extra pure cobalt carbonate (Himedia) and LR grade ferric oxide (Thomas Baker). These materials were weighed in the required stoichiometric proportion, mixed and milled in agate mortar with acetone. The mixture of powder was pre-sintered at  $600\text{ }^\circ\text{C}$  for 10 h. The pre-sintered powders were milled to have a fine powder and sintered at  $1000\text{ }^\circ\text{C}$  for 24 h. The sintered powder was milled with acetone and 10% poly vinyl alcohol and pressed in the form of pellets of diameter 10 mm with a pressure of about  $5\text{ ton/cm}^2$  using hydraulic press machine. The pellets were sintered at  $1000\text{ }^\circ\text{C}$  for 2 h. The heating and cooling of the samples were carried out at  $80\text{ }^\circ\text{C/h}$ .

The X-ray diffraction patterns were recorded at a step size of 0.02 in angular range of  $10\text{--}100^\circ$  ( $2\theta$ ) at 40 kV and 25 mA with  $\text{Cr-K}\alpha$  radiation ( $\lambda = 2.29165\text{ \AA}$ ) using Philips PW-3710 X-ray powder diffractometer. FTIR spectrum was recorded in the range of  $350\text{--}800\text{ cm}^{-1}$  using Perkin-Elmer spectrum one spectrophotometer, USA. Scanning electron microscopy was carried out to analyse the microstructure of fractured surfaces of the pellets using JEOL JSM 6360 SEM model (Japan).

### 3. Results and discussion

The X-ray diffraction patterns of  $\text{Cd}_x\text{Co}_{1-x}\text{Fe}_2\text{O}_4$  ( $x = 0.80, 0.85, 0.90, 0.95$  and  $1.0$ ) system are presented in figure 1. The presence of (220), (311), (422), (333) and (440) planes in the patterns confirms the formation of single phase cubic

\*Author for correspondence (sanjeevdalawai@gmail.com)

spinel structure. The (311) peak in the diffraction patterns agrees with JCPDS card number 02-0975. Lattice constant of all the samples under investigation is calculated using the Bragg's equation (Cullity and Stock 2001)

$$a = d_{hkl} \sqrt{h^2 + k^2 + l^2}, \quad (1)$$

where  $d_{hkl}$  is the interplaner distance and  $(h, k, l)$  are the Miller indices. The variation of lattice constant with cadmium content of  $\text{Cd}_x\text{Co}_{1-x}\text{Fe}_2\text{O}_4$  ( $x = 0.80, 0.85, 0.90, 0.95$  and  $1.0$ ) system is presented in figure 2. From this figure, it

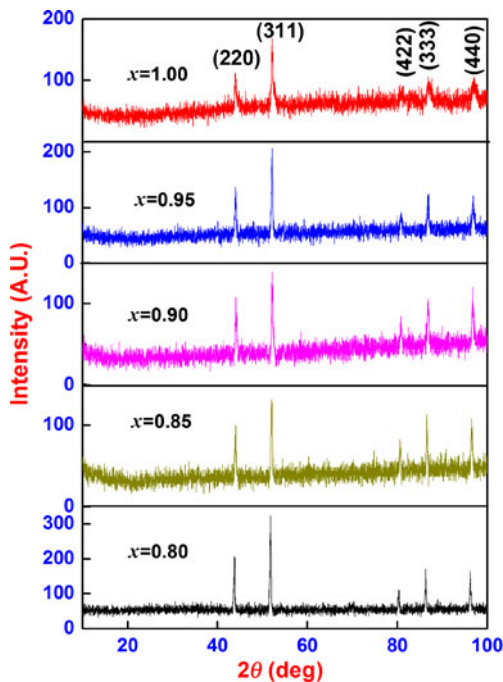


**Figure 1.** XRD patterns of  $\text{Cd}_x\text{Co}_{1-x}\text{Fe}_2\text{O}_4$  ( $x = 0.80, 0.85, 0.90, 0.95$  and  $1.00$ ).

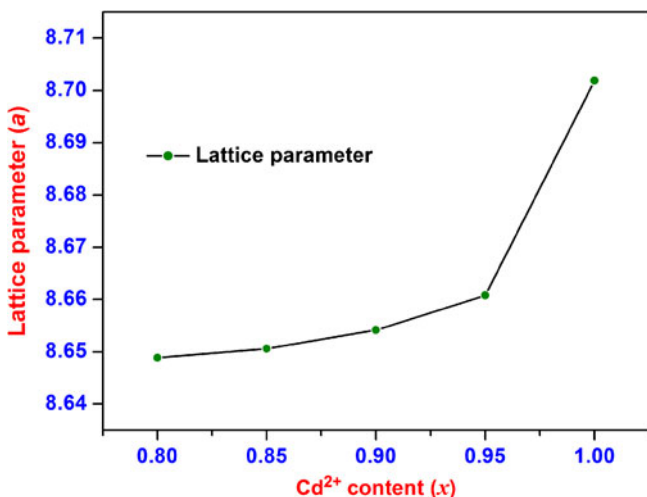


**Figure 2.** Variation of lattice constant with  $\text{Cd}^{2+}$  content in  $\text{Cd}_x\text{Co}_{1-x}\text{Fe}_2\text{O}_4$  ( $X = 0.80, 0.85, 0.90, 0.95$  and  $1.00$ ).

is observed that the lattice constant increases with increase in  $\text{Cd}^{2+}$  content. This is attributed to replacement of smaller ionic radii Co ( $0.78 \text{ \AA}$ ) by larger ionic radii  $\text{Cd}^{2+}$  ( $0.99 \text{ \AA}$ ) ions. Similar behaviour of lattice constant with cadmium content is also reported by Abdeen *et al* (2002) and Gabal and Ata-Allah (2004).

The average crystallite size of the samples was calculated from the (311) peak of XRD by using Debye–Scherrer formula (Cullity and Stock 2001)

$$D = \frac{0.94\lambda}{\beta \cos \theta}, \quad (2)$$

where  $\lambda$  is the wavelength of the X-ray,  $\beta$  the full width at half maximum and  $\theta$  the Bragg's angle. The crystallite size of all the samples lies in the range of  $29.1\text{--}42.8 \text{ nm}$  and is presented in table 1. The physical density ' $\rho_p$ ' of the sample was determined by the Archimedes principle using the relation:

$$\rho_p = \left( \frac{w}{w - w'} \right) \rho, \quad (3)$$

where  $w$  is the weight of the sample in air,  $w'$  the weight of the sample in xylene and  $\rho$  the density of xylene. The physical density of all the samples under investigation is presented in table 1.

The bond lengths (A–O and B–O) and ionic radii ( $r_A$  and  $r_B$ ) on A-site and B-site are calculated using the equation (Standley 1972),

$$\text{A–O} = (u - 1/4) a \sqrt{3}, \quad (4)$$

$$\text{B–O} = (5/8 - u) a, \quad (5)$$

$$r_A = (u - 1/4) a \sqrt{3} - r(\text{O}^{2-}), \quad (6)$$

$$r_B = (5/8 - u) a - r(\text{O}^{2-}). \quad (7)$$

The calculated values of bond lengths and ionic radii on A-site and B-site are presented in table 1. From this table, it is observed that bond length (A–O) and ionic radii on ( $r_A$ ) on A-site increase with increase in  $\text{Cd}^{2+}$  content. This is attributed to the increase in lattice constant with increase in  $\text{Cd}^{2+}$  content in the system under investigation. The bond lengths (B–O) and ionic radii ( $r_B$ ) on B-site decrease with increase in  $\text{Cd}^{2+}$  content.

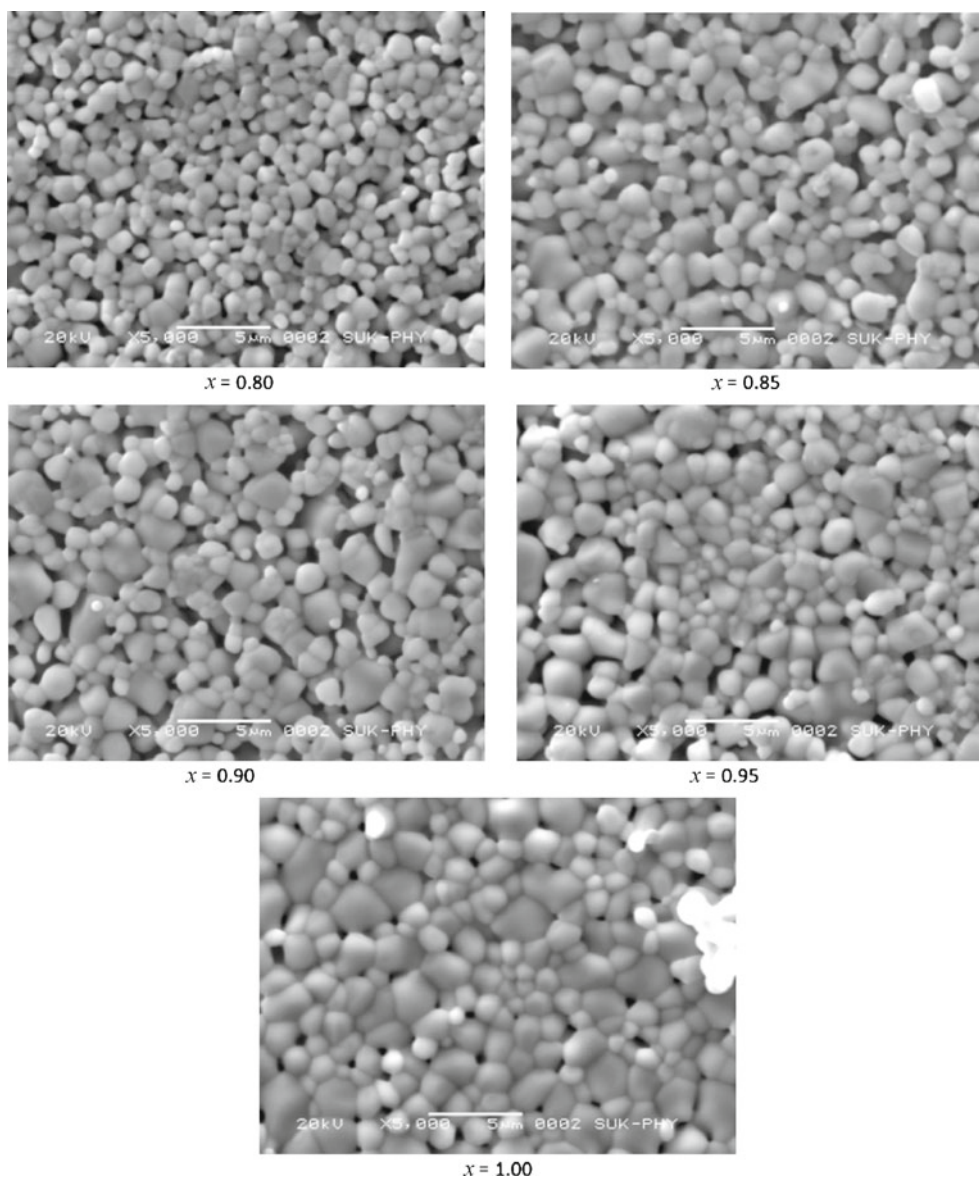
The microphotographs of fractured surface of  $\text{Cd}_x\text{Co}_{1-x}\text{Fe}_2\text{O}_4$  ( $x = 0.80, 0.85, 0.90, 0.95$  and  $1.00$ ) system are presented in figure 3. The grain size is calculated by linear intercept method using the formula (Wurst and Nelson 1972),

$$G_a = \frac{1.5L}{MN}, \quad (8)$$

where  $L$  is total test line length,  $M$  the magnification and  $N$  the total number of intercepts. The morphology of particles is almost spherical and regular in shape and uniform.

**Table 1.** Structural parameters of  $\text{Cd}_x\text{Co}_{1-x}\text{Fe}_2\text{O}_4$  ( $x = 0.80, 0.85, 0.90, 0.95$  and  $1.00$ ) system.

Cd <sup>2+</sup> content, $x$	Crystallite size, $D$ (nm)	Grain size, $G_a$ ( $\mu\text{m}$ )	X-ray density, $\rho_x$ (g/cc)	Physical density, $\rho_p$ (g/cc)	Porosity, $p$ (%)	Bond length ( $\text{\AA}$ )		Ionic radii ( $\text{\AA}$ )		FTIR absorption bands ( $\text{cm}^{-1}$ )	
						A–O	B–O	$r_A$	$r_B$	$\nu_1$	$\nu_2$
						0.80	42.8	0.83	5.591	2.792	50.05
0.85	38.6	1.00	5.726	3.109	45.69	2.065	2.055	0.715	0.705	553.00	438.00
0.90	33.5	1.11	5.819	3.119	46.38	2.067	2.047	0.717	0.696	555.87	436.80
0.95	39.1	1.25	5.856	2.945	49.69	2.076	2.045	0.726	0.695	559.00	420.00
1.00	29.1	1.66	5.914	3.529	40.33	2.082	2.041	0.732	0.691	562.84	416.69

**Figure 3.** Micrographs of  $\text{Cd}_x\text{Co}_{1-x}\text{Fe}_2\text{O}_4$  ( $x = 0.80, 0.85, 0.90, 0.95$  and  $1.00$ ).

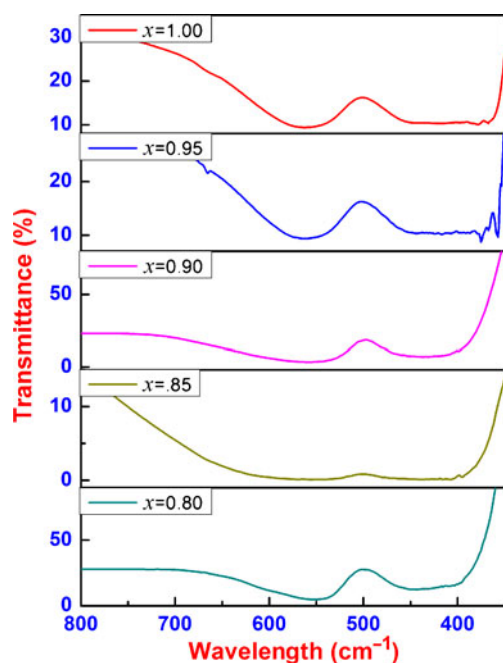


**Figure 4.** FTIR spectra of  $\text{Cd}_x\text{Co}_{1-x}\text{Fe}_2\text{O}_4$  ( $x = 0.80, 0.85, 0.90, 0.95$  and  $1.00$ ).

The grain size of the samples is presented in table 1. It shows that the grain size increases with increase in  $\text{Cd}^{2+}$  content. Similar result is reported for  $\text{Cd}^{2+}$  substituted Mg ferrites (Gadkari et al 2010).

The infrared spectra of  $\text{Cd}_x\text{Co}_{1-x}\text{Fe}_2\text{O}_4$  ( $x = 0.80, 0.85, 0.90, 0.95$  and  $1.00$ ) system are shown in figure 4. The spectra show two major absorption bands near about  $400\text{ cm}^{-1}$  and  $600\text{ cm}^{-1}$  of octahedral and tetrahedral sites, respectively. The higher absorption band ( $\nu_1$ ) and lower absorption band ( $\nu_2$ ) are assigned to the tetrahedral and octahedral sites (Waldron 1955). The values of absorption bands ( $\nu_1$  and  $\nu_2$ ) corresponding to tetrahedral and octahedral sites are presented in table 1. It is observed that absorption band ( $\nu_1$ ) goes on increasing while absorption band ( $\nu_2$ ) decreases with increase in  $\text{Cd}^{2+}$  content. The difference in frequencies of  $\nu_1$  and  $\nu_2$  is due to changes in the bond length  $\text{Fe}^{3+}-\text{O}^{2-}$  at tetrahedral and octahedral sites. IR spectroscopy for several ferrites were reported (Waldron 1955).

The nature of absorption bands in the infrared spectra depends on the distribution and type of cations among octahedral and tetrahedral sites (Modi 2004).

#### 4. Conclusions

X-ray diffraction analysis confirms the formation of single phase cubic spinel structure of Cd–Co ferrites. The lattice constant is found to be increasing with increase in  $\text{Cd}^{2+}$  content. The crystallite size of the samples lies in the range of 29.1–42.8 nm. The infrared absorption study shows two absorption bands around  $400$  and  $600\text{ cm}^{-1}$  corresponding to tetrahedral and octahedral sites. The values of absorption bands  $\nu_1$  increase whereas  $\nu_2$  band decrease with  $\text{Cd}^{2+}$  content. The grain size of the samples increases with increase in  $\text{Cd}^{2+}$  content.

#### Acknowledgement

The authors are grateful to the University Grants Commission, New Delhi, for the financial assistance extended through the major research project Ref. No. F. No. 36-212/2008 (SR).

#### References

- Abdeen A M, Hemeda O M, Assem E E and El-Sehly M M 2002 *J. Magn. Magn. Mater.* **238** 78
- Cullity B D and Stock S R 2001 *Elements of X-ray diffraction* (New York: Prentice Hall) p. 154
- Gabal M A and Ata-Allah S S 2004 *Mater. Chem. Phys.* **85** 104
- Gadkari A B, Shinde T J and Vasambekar P N 2010 *J. Mater. Sci. Mater. Elect.* **21** 96
- Gaikwad R S, Chae S Y, Mane R S, Han S H and Joo O S 2011 *Int. J. Electrochem.* **2011** 1
- Modi K P 2004 *Proc. Indian Acad. Sci.* **62** 1173
- Nikumbh A K, Nagawade A V, Tadake V B and Bakare P P 2001 *J. Mater. Sci.* **36** 653
- Standley K J 1972 *Oxide magnetic materials* (Oxford, UK: Clarendon)
- Vasambekar P N, Kolekar C B and Vaingankar A S 1999 *J. Mater. Sci. Mater. Elect.* **10** 667
- Waldron R D 1955 *Phys. Rev.* **99** 1727
- Wurst J C and J A Nelson 1972 *Am. Ceram. Soc. Bull.* **55** 109